Diversion of the River Neva

How will it Influence the Baltic Sea, the Belts and Cattegat

Flemming Bo Pedersen and Jacob Steen Møller

Technical University of Denmark, Copenhagen

Diverging part of the river Neva discharge to the dry regions in the southern USSR has raised the question, to what extent such a river diversion will influence the hydrographic conditions in the Baltic Sea and the Danish Inland waters. In order to quantify the influence, the system has been divided into eight subareas, each of which is characterized by an equation for the mass, the volume and the dynamic balance (the mixing), respectively. The man-made change in the river runoff has been introduced in the equations, which have then been linearized and solved with respect to changes in the salinities, the discharges and the layer depths in the system.

As a quantitative example the hydrographic consequences of a 25% reduction in the river Neva discharge have been outlined. The most pronounced influence is on the salinities, which are increased by 0.2 to 0.4 ‰ allover in the system. Hence, if the river diversion had become executed in the beginning of this century a 30 to 40% higher salinity-variation would have been encountered in the Baltic Sea – compared to the actual variations during this century.

Introduction

The increasing water demand for irrigational purposes in the dry regions north of the Caspian Sea and the Lake Aral (in the USSR) has actualized the plans of pumping huge amounts of water from the catchments of the river Ob and the river Neva to the river Volga, which are running through the affected dry areas. The USSR's Council of Ministers have, in fact, in their 5-year plan 1976-80 initiated the preliminary planning for diverging up to 2,000 m³/s from the river Ob, which

1

drains to the Arctic Sea. Although not mentioned directly in the available sparse information on the project, Mikhaylow et al. (1977), Voropaev (1978), Golubev (1978), it is obvious from an engineering point of view, that the river Neva is also attractive as a source to this irrigation project. With a discharge of approximately 3×10^3 m^3/s, the river Neva is the largest single fresh water contributor to the Baltic Sea, to which the total average fresh water input is, in the order of 15×10^3 m^3/s. Therefore, a radical decrease in the runoff from the river Neva has a great bearing on the hydrography of the Baltic. Further, it has also a large effect on the hydrography of the inland Danish waters, which links the brackish Baltic Sea to the ocean.

A man-made regulation of the river Neva is therefore a matter of international concern, as it will influence all the countries boardering the Baltic. On the other hand, there seems to be no international laws or conventions, which makes it possible for the other Baltic countries to change the decisions if possibly unwanted effects of the regulations can be foreseen. The problem has a parallel in the Danish project for building a bridge across the Great Belt, which was estimated to have a measureable influence on the Baltic Sea, Bo Pedersen (1978). Although there was an international reaction against the building of the bridge, it was for economic reasons, that the Danish government finally decided to postpone the bridge project.

The main objective of the present paper is to establish an estimate of the hydrographic changes in the Baltic Sea and the Danish inland waters if part of the river Neva's discharge is diverged from the Baltic Sea. An evaluation or estimation of the possible consequences for the affected countries is beyond the scope, but it is the hope, that the article will act as a trigger for further discussions, and that the findings will serve as a basis for further work.

The Basic Principles and Assumptions for the Model

In the Baltic Sea and its connections with the North Sea (the Cattegat, the Belts and the Sound) all types of estuaries, i.e. semienclosed bodies of water, where a measurable dilution by fresh water are present, can be recognized. Although a throughout hydrographic description of an estuary demands knowledge of the variation in space and time of all relevant physical properties, such as salinity, temperature, oxygen content, phosphate and nitrate concentrations etc. we shall make a common approach and restrict ourselves to a representative *steady-state* situation considering only the *salinity* distribution, which is the property governing the vertical stability and hence the mixing in the actual case. The most simple representation of an estuary in which the basic physical conditions are maintained is a *two-layer* flow. An inspection of the actual conditions in the Baltic Sea and in the Danish inland waters confirms, that this is a fair approximation.

Our approach is then, first to identify the major external forces affecting the

system (fresh water discharge, wind, tide, etc.), then to estimate the correct order of magnitude of the strength of these forces, introduce them in our model and then finally confirm with the actual measured conditions in the estuary, that our model is reasonable representative for the dynamics of the estuary. After the verification of the model, we introduce the change in the fresh water discharge from the river Neva – linearize the equations – and solve with respect to the changes in the salinities, the depths and the flows in the idealized estuaries. In these calculations we have focused on the man-made changes in the fresh water discharge. The consequences for the layer depths and salinities in the Baltic Sea for a natural variation in the fresh water discharge are different from our findings, due to the strong correlation between the precipitation (and hence the runoff) and the meteorological conditions, the last being held unchanged in our calculations.

As stated above all types of estuaries are present in the model. The dynamics of an estuary is mainly affected by the following parameters, Bo Pedersen (1980a)

1. The geometry
2. The hydrology of the adjacent watershed
3. The oceanographic conditions outside the estuary
4. The wind field (and the barometric pressure variation due to the large dimensions of the Baltic Sea).

The great variability of these parameters over the actual oceanographic field makes it necessary to divide the total area into eight subareas as indicated in Fig. 1. The subdivision is chosen in such a way that a reasonable simple dynamic description can be given for each region, and hence, the areas do not represent regions of equal importance, merely areas of different dynamic behaviour.

For each subarea steady-state continuity-equations for mass and volume are established. One of the terms of major importance for the continuity equations, is the term representing the mixing accross the interface separating the two layers. This mixing is due to the generation of turbulence by external forces, such as tide, variable meteorological conditions, etc., i.e. all highly non-stationary forces. Therefore, although the basic objective is to establish a steady-state model, it is necessary to incorporate the non-steady dynamic behaviour of the system in the description in order to maintain the correct physics. To transfer a dynamic situation to an artificial steady state demands knowledge of the representative time scale and the representative force scale. With focus on the mixing, a representative averaging time scale is the residence time, T, i.e. a measure of the mean time that a particle of tracer remains inside the actual subarea of the estuary system

$$T = \frac{Vol}{Q} \tag{1}$$

where *Vol* is the total volume of pure fresh water inside the subarea and Q is the accumulated fresh water discharge at the actual cross section. The residence time for the Baltic estuary system varies from for example, typically a week in the Belt

3

s [km]   τ_w   1500   1000   R   500   0

Index 0

Index 1

K   S   A   B

MK   KS   SA   AB   BC   C   Ø   F

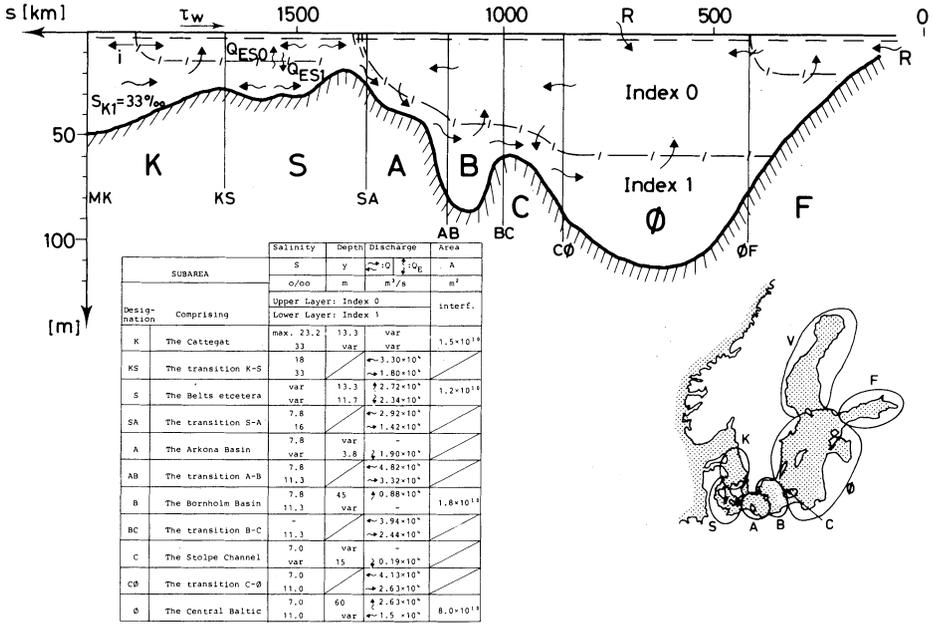| SUBAREA		Salinity S o/oo	Depth y m	Discharge Q_E m³/s	Area A m²
Designation	Comprising	Upper Layer: Index 0 / Lower Layer: Index 1			interf.
K	The Cattegat	max. 23.2 / 33	13.3 / var	var / var	1.5×10¹⁰
KS	The transition K-S	18 / 33		←~3.30×10⁴ / ~→1.80×10⁴	
S	The Belts etcetera	var / var	13.3 / 11.7	↑2.72×10⁴ / ↓2.34×10⁴	1.2×10¹⁰
SA	The transition S-A	7.8 / 16		←~2.92×10⁴ / ~→1.42×10⁴	
A	The Arkona Basin	7.8 / var	var / 3.8	1.90×10⁴	-
AB	The transition A-B	7.8 / 11.3		←~4.82×10⁴ / ~→3.32×10⁴	
B	The Bornholm Basin	7.8 / 11.3	45 / var	↑0.88×10⁴	1.8×10¹⁰
BC	The transition B-C	- / 11.3		←~3.94×10⁴ / ~→2.44×10⁴	
C	The Stolpe Channel	7.0 / var	var / 15	↓0.19×10⁴	-
CØ	The transition C-Ø	7.0 / 11.0		←~4.13×10⁴ / ~→2.63×10⁴	
Ø	The Central Baltic	7.0 / 11.0	60 / var	↑2.63×10⁴ / ←1.5×10⁴	8.0×10¹¹

Fig. 1. The Baltic estuary system divided into eight subareas. The specific hydrodynamic characteristics of the six outermost subareas are summarized in the table.

region, a month in the Cattegat region to 30 years at the central Baltic. As the time scale for the tide (a day) as well as for an average meteorological event (a week) are below the averaging time for the estuary, these two types of external forces can in the time frame be treated as steady, persistent forces, although it may be admitted, that the seasonal variations as for instance in the meteorological activity and in the runoff cannot be incorporated in our theory. On the other hand, the seasonal variations are much weaker than the single events, and can therefore be neglected in the analysis. The other important scale for the mixing is the force scale, i.e. a measure for the energy available for the mixing process. This is the subject of the next chapter.

Mixing in a Two-Layer Stratified Flow

The two-layer stratified flow is characterized by having two nearly homogeneous layers separated by an interface with a sharp density gradient. The mixing between the two layers can be treated as pure (one-way) entrainment if the level of kinetic energy is high in the one layer and negligible in the other layer. If a measurable level of kinetic energy is present in both layers a two-way transport exists, which can be treated either as a combined entrainment/diffusion problem or, as we prefer it, as a double-sided entrainment. A comprehensive analysis of

4

the entrainment functions for a large class of two-layer flows can be found in Bo Pedersen (1980a). The basic assumption for all the flow cases treated there is, that a universal relationship exists between the energy available for the turbulence (i.e. the production with some minor corrections) and the energy gained (potential as well as turbulent kinetic energy) due to the entrained mass. Hence, the characteristic force scale for the mixing, i.e. for the entrainment, can be evaluated by taking a moving average value of the energy input into the system, which by Bo Pedersen (1980a) is shown to be proportional to the mean speed in the layer $|v|$ to the third power. Hence, the proper dynamic transformation from the non-steady to the steady system is done by applying a mean velocity $\tilde{V}$ defined by

$$\tilde{V} = (\frac{1}{T} \int_0^T |v|^3 dt)^{\frac{1}{3}} \tag{2}$$

The velocity scale in the continuity equation is the simple mean velocity and not the velocity defined by Eq. (2). It is therefore necessary to incorporate a circulation-velocity with no net transport inside some of the regions in order to get dynamic- as well as mass-balance in the simplified systems.

The major external forces producing turbulence in the system are:

1. *The wind,* which generates a flow in the upper layer. A persistent wind acting far from boundaries causes an entrainment velocity V_E which can be evaluated by the following equation, Bo Pedersen (1980a)

$$\frac{V_E}{U_F} = \frac{2.3}{6 + \mathbb{R}i_F} \qquad \mathbb{R}i_F = \frac{\Delta gy}{U_F^2} \tag{3a}$$

where $U_F = (\tau_W/\varrho)^{1/2}$ is the friction velocity in the water due to the windstress τ_W. The bulk Richardson number $\mathbb{R}i_F$ is a measure of the stability of the system as Δ is the non-dimensional density difference between the upper and the lower layer ($\Delta\varrho = \varrho_{lower} - \varrho_{upper}$), g is the acceleration of gravity and y the upper layer depth. All the subareas in the Baltic have rather stable interfaces, i.e. $\mathbb{R}i_F >> 6$, which means that Eq. (3) can be reduced to

$$\frac{V_E}{U_F} \simeq \frac{2.3\ U_F^2}{\Delta gy} \tag{3b}$$

2. *The heating/cooling* process forms during the summertime a stable thermocline. In the winter period it creates an unstable free convection, which erodes the thermo- or halocline.

As shown by Bo Pedersen (1980a) it is only in those parts of the Baltic system, where the halocline is located deep (Bornholm Basin $y \simeq 45$ m, Baltic Proper $y \simeq 60$ m), that a thermocline forms during a pronounced period of the year. The thermocline acts as a lid, which prevents the wind from creating mixing through

5

the halocline – in the actual region during nearly half a year, which has to be taken into account in the dynamical part of the calculations. During the thermocline-free period the free convection plays the minor role in the overall erosion of the halocline. Therefore the only influence from the heating/cooling in our simple model is, that it prevents mixing in the Bornholm Basin and in the Baltic Proper during half a year.

3. *The tide* generates a periodic in and out flow, which can be registrated in the Danish inland waters. On the other hand, the energy input into the system from the tide is sufficiently small to be negligible in the present analysis.

4. *The meteorological activities* over Scandinavia with succeeding low and high pressure acts like a piston on the Baltic Sea. Combined with wind set-up and set-down an oscillating in- and out-flow through the Danish inland waters is generated. In the Cattegat, the Belts and the Sound this means that a large part of the surface and the bottom water is pendling in an out producing turbulent kinetic energy and therefore mixing. The other type of mixing, which shall be considered, occurs in the Arkona region where the pendling only takes place in the surface water. The saline bottom water is trapped in a dense bottom current on the eastern slope of the Darss Sill (16 m depth) in the Great Belt and on the southern slope of the Drogden Sill (8 m depth) in the Sound.

The order of magnitude of the non-steady flow in the Cattegat and the Belts can be evaluated from the discharge measurements performed in the Great Belt, reported by Jacobsen (1980), see Fig. 2. The typical amplitude in the pendling is about $10^5 m^3/s$, which is 10 times the average fresh water outflow through the Great Belt. This ratio between the mass average and the dynamic average velocity demonstrates the presence of a large no net flow circulation.

The circulation induced mixing can be treated as a quasi-steady mixing due to the extreme large ratio between the non-steady period of the circulation (weeks) and the mixing time scale (hours). For a steady-state condition the strength of the circulation induced entrainment to the wind induced entrainment can be shown (Bo Pedersen 1980a) to be equal for a ratio of the dynamic mean velocity $\tilde{V}$ to the wind generated friction velocity U_F of

$$\frac{\tilde{V}}{U_F} \simeq 50 \tag{4}$$

In the Cattegat a typical high front speed is $V \simeq 0.1$ m/s, while the representative dynamic friction velocity due to the wind is $U_F \simeq 8 \times 10^{-3}$m/s. Hence in Cattegat the circulation contribution to the mixing is only a few per cent of the wind generated mixing and can therefore be neglected.

In the Belts the typical observed velocities are of an order of magnitude which makes them just as important for the mixing process as the wind, i.e. $V \simeq 0.4$ m/s.
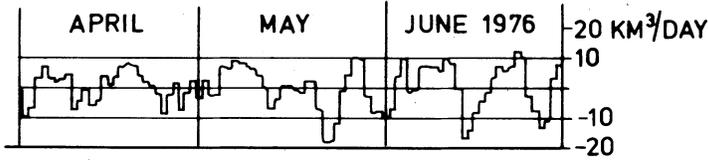
6

Fig. 2. Typical time series of the measured outwards (positive) and inwards discharge through the Great Belt. From Bo Pedersen (1978).

Fortunately for the present analysis the circulation as well as the wind do both originate from the meteorological activity over Scandinavia, which is kept unchanged in the analysis. The above-mentioned theory considering the ratio between the gain in energy due to entrainment to the production of turbulent kinetic energy simply states for the Belts, that the volume of entrained water Q_{EO} amounts to

$$Q_{E0} = \frac{A \cdot constant}{(S_{S1} - S_{S0})y_{S0}} \tag{5}$$

The constant in the numerator stands for the dynamic turbulence production and is estimated below. The denominator represents the gain in potential energy of the entrained mass, namely proportional to the salinity difference (the paranthesis) and the upper layer depth. The high velocities in the non-stationary flow in the Belts creates a downwards as well as an upwards directed entrainment. Again – using the efficiency concept for the mixing – the downwards entrainment is similar to the upwards entrainment discharge

$$Q_{E1} = \frac{A \cdot constant}{(S_{S1} - S_{S0})y_{S1}} \tag{6}$$

where the constant stands for the dynamic energy input and y_{S1} is the lower layer depth in the Belts.

The dense bottom current in the Arkona Basin is a highly intermittent flow (Bo Pedersen 1977, Petrén and Walin 1975), which only takes place in connection with an inflow situation to the Baltic. The other dense bottom current in the system – from the Bornholm Basin through the Stolpe Channel into the Baltic proper – is a nearly persistent flow, due to the reservoir effect of the Bornholm Basin (Bo Pedersen 1977, Rydberg 1976). Dense bottom currents in a rotating coordinate system has been treated in Bo Pedersen (1980b). The discharge Q as a function of the distance s along the pathline of the flow is increasing due to entrainment, such that

$$Q(s) = Q(s=0) \exp\{0.072 \int_0^s \frac{I \, ds}{y}\} \tag{7}$$

7

where I is the local bottom slope. As the depth y is nearly independent of the distance, the integral simply is the drop in elevation non-dimensionalized by the depth. For an unchanged geometry it can furthermore be expected, that the densimetric Froude's number at the sill is unchanged too, see Bo Pedersen (1980a and b), i.e.

$$(\frac{Q^2}{\Delta g B^2 y^3})_{\text{before}} = (\frac{Q^2}{\Delta g B^2 y^3})_{\text{after}} \tag{8}$$

where the indexes before/after relates to the change of the river Neva discharge into the Baltic Sea.

Characteristics of the Subareas

With the major external forces identified and the associated mixing processes quantified, a description of the individual subareas can be given, including the equations governing the mass and the volume balances and the dynamic behavior. Furthermore, we shall try to a certain extent to verify the simple models presented, against field measurements. To facilitate these assessments a summarizing chart is given, Fig. 1, which contains the symbols used and the values adapted in the present approach to the problem. Finally a summary scheme is given, which contains all the equations needed for the final calculation. The initial values attributed the salinities, the depths and the discharges (see Fig. 1) all satisfy the outlined equations, and are therefore consistent with our interpretation of the dynamics of the system.

Subarea 1: The Cattegat

The western part of the approximately 100 km wide and 240 km long Cattegat has an average depth of approximately 10 m, which is less than the nearly constant upper layer depth in the permanent salt water wedge present in the eastern part, where the total depth is up to 100 m. Hence in the shallow western part a well mixed estuary is normally present, while the eastern part has the characteristics of a two-layer salt water wedge, with constant salinity in the lower layer and varying upper layer salinity.

According to our model, the mixing in the Cattegat is primarily upwards directed entrainment caused by the energy input from the wind. With reference to Fig. 1 the continuity equation for volume states

$$Q_{K0} = Q_{KS0} + \int_0^x V_{EK} B_K \, dx \tag{9}$$

where Q_{K0} is the upper layer net discharge in position x, and Q_{KS0} is the southern boundary value of this discharge (B_K = the interfacial width). The mass deficit

8

flux is constant, because the lower layer salinity is constant and because the mixing is pure upwards directed entrainment. Hence

$$Q_{K0} \Delta_K = Q_{KS0} \Delta_{KS} \tag{10}$$

where Δ_K and Δ_{KS} stands for the non-dimensional mass deficit at position x and at the southern boundary, respectively.

The dynamic conditions in the Cattegat is described by an entrainment function, Eq. (3b) as well as a boundary condition at the northern boundary, where a front is present. In lack of detailed knowledge of the dynamics of this front a common, simple front condition has been used, namely that the densimetric Froude number $\mathbb{F}_\Delta$ at the front is a constant, i.e.

$$\mathbb{F}_\Delta^2 = \frac{Q^2}{\Delta g B^2 y^3} = \text{constant} \tag{11}$$

where the discharge Q stems from the oscillatory flow.

Eqs. (9), (10) and (3b) can be solved to yield the density-deficit distribution in the Cattegat

$$\frac{1}{\Delta_K} = \frac{1}{\Delta_{KS}} \exp\left(\frac{x}{\lambda_K}\right) \tag{12}$$

where the length scale λ_K is determined by

$$\lambda_K = \frac{\Delta_{KS} \, g \, y_{K0} Q_{KS0}}{2.3 \, B_K \, U_F^3} \tag{13}$$

If we introduce the empirical relation between the deficits in the density ϱ and the salinities

$$\rho_1 - \rho_0 \simeq 0.75 \, (S_1 - S_0) \tag{14}$$

Eq. (1) can be transformed to

$$S_{K1} - S_{K0} = (S_{K1} - S_{KS0}) \exp\left(\frac{1,680 \cdot 10^3 - s}{\lambda_K}\right) \tag{15}$$

where s (in m) is the overall stationing which starts at the head of the Bothnian Bay (at the Neva inlet to the Bay) and end at the Cattegat/Skagerack front where $s = 1,920 \times 10^3$ m (s = $1,680 \times 10^3$ m corresponds to the Belt/Cattegat transition), and λ_K takes the value 565×10^3 m.

Eq. (15) describes an equivalent steady, yearly averaged salinity-distribution in the upper layer of the Cattegat. This layer is in fact subject to great forwards and backwards movements during the year. Hence Eq. (15) cannot be checked by field measurements before it has been modified slightly. The non-steady movements are reflected in the position of the Cattegat front, which during an inflow situation moves towards the Belts. North to the front the saline Skagerack water is

9

encountered (salinity $\approx 33\%_0$) – south to the front the brackish Cattegat water is present. The front movements have been simulated by Møller (1980) for half a year during 1975 by applying continuity considerations based on the observed in- and outflows through the Belts (Jacobsen 1980), which was estimated to account for 60% of the total flow. From these calculations an intermittency function can be outlined, where the intermittancy i is defined as the proportion of the total time in which the front is located north to the actual section. Assuming a Poisson distribution for i, we have

$$i = 1 - \exp\left(\frac{s-1,920\cdot10^3}{L_K}\right) \tag{16}$$

where $L_K = 40 \times 10^3$ m is the average inwards movement of the front.

In summary: In order to check the outlined salinity distribution with the salinities encountered in the Cattegat, we have to take the front movements into account, which yield an apparent salinity distribution

$$\overline{S_{K0}} = S_{K0}\,i + S_{K1}(1-i) \tag{17}$$

where $\overline{S_{KO}}$ is the yearly average salinity in the upper layer of the Cattegat. In Fig. 3 is shown the observed and the calculated yearly averaged salinities. The figure confirms the usefulness of the simple description, especially when it is realized that no »curve-fitting« is used in order to obtain agreement.

Subarea 2: The Belts
The hydrodynamics of subarea 2, which comprises the Belts, the Sound and the Kieler Bay are extremely complicated mainly due to the shallowness of the area (depth of 20 m to 30 m) combined with the highly non-steady in- and outflow of huge amounts of stratified brackish water. On an average a two-layer system exists. The existence of a salinity variation in the upper as well as in the lower layer shows that two-way entrainment is present, which agree with the lower layer being dynamical active in this region. A comprehensive description of the hydro-graphy (inclusive some considerations on the dynamic conditions) of subarea 2 can be found in The Belts project (1976), DHI report (1977) Bo Pedersen (1978) and Jacobsen (1980) where further references to the subject are given. Based on these findings (see also Fig. 2) we assume, that a typical flow cyclus representative of the present consequence analysis is as illustrated in Fig. 4, namely a net out-wards flow due to the fresh water discharge R super-imposed by an oscillatory motion with an amplitude in accordance with the measurements, i.e. approxima-tely a factor of ten times R. The amplitude and the frequency of the cyclus is governed by the meteorologic conditions as the forcing and the friction as the damping factors. As demonstrated by Bo Pedersen (1978), the total flow resistan-ce for the upper layer in the Great Belt is at its minimum at the present average
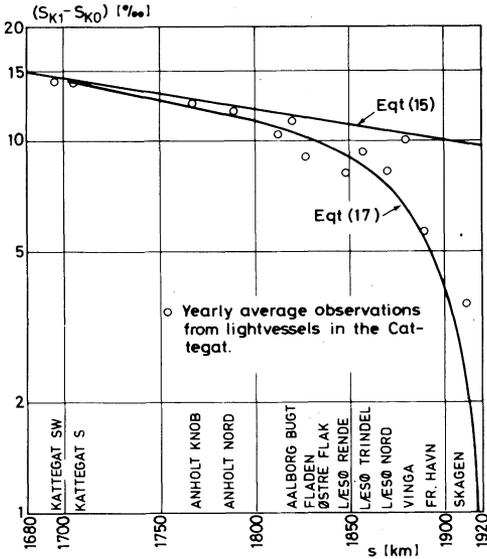
10

Fig. 3. Calculated and observed yearly average salinity differences between lower (S_{K1}) and upper (S_{K0}) layer in the Cattegat. Eq. (15) illustrates the calculated variation not taking the intermittancy into account (the front movements). Eq. (17) takes the intermittancy into account.

cyclic flow conditions, and hence a minor man-made change in the fresh water discharge will neither create changes in the amplitude nor in the frequency of the pendling discharge, see Fig. 4. Furthermore the minimum condition implies that no change in the production of turbulent kinetic energy occurs.

The sills which separate the Belts and the Sound from the Arkona Basin trap the inwards flowing water which descends as a dense bottom current into the lower layer of the stratified Bornholm Basin, see Fig. 1. If we assume, that the time in which trapping occur is nearly independent of the fresh-water discharge,
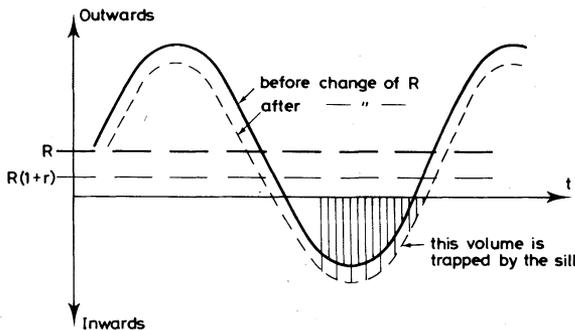

Fig. 4. The inflow/outflow through the Belts schematized by a simple harmonic cyclus superimposed on the fresh-water runoff. The volume trapped by the sills is hatched.

11

the following simple equation for the sill overflow Q_{SA1} (see Fig. 4) applies

$$Q_{SA1} + R = \text{const}_{SA1} \tag{18}$$

The other equations describing the model outlined are the continuity equations, which are

$$S_{K0}(Q_{ES0} - Q_{ES1} + Q_{SA1} + R) = S_{K1}(Q_{ES0} - Q_{ES1} + Q_{SA1}) \tag{19}$$

stating the no net transport of salt condition at the Belts/Cattegat transition, and

$$S_{SA1}Q_{SA1} = (Q_{ES0} - Q_{ES1} + Q_{SA1})S_{K1} - Q_{ES0}S_{S1} + Q_{ES1}S_{S0} \tag{20}$$

expressing the salt balance for the lower layer in the Belts. The entrainment fluxes (the Q_E's) are as stated in the previous chapter related to the dynamics of the flow, Eqs. (5) and (6). The salinities S_{S1} and S_{S0} in the upper and the lower layer, respectively are for conveniency taken as simple averages of the boundary values, i.e.

$$S_{S0} = 0.5(S_{KS0} + S_{SA0})$$
$$S_{S1} = 0.5(S_{KS1} + S_{SA1}) \tag{21}$$

The complexity of the flow pattern and of the geometry makes it a rather difficult task to give a convincing verification of the outlined Belt model, but a check can be made by considering some reasonable values for the measured/estimated quantities. Inserting the values shown in Fig. 1 in the governing equations yields

$$Q_{ES0} = 2.72 \cdot 10^4 \text{ m}^3/\text{s}$$
$$Q_{ES1} = 2.18 \cdot 10^4 \text{ m}^3/\text{s} \tag{22}$$

The upwards directed entrainment Q_{ES0} can be compared with the entrainment one would have had, if it was purely wind generated (see Eq. (3b)). With an interfacial area of approximately 10^{10} m^2 Eq. (3b) gives an upwards entraining flux of 1.2×10^4 m^3/s. The remaining entrainment, 1.5×10^4 m^3/s, can be accounted for by an upper layer dynamic velocity of $\tilde{V} \simeq 0.45$ m/s (see Bo Pedersen 1980a) which is in good agreement with the prevailing flow conditions in the main contributor, the Great Belt. The downward entrainment is created by the turbulence production in the lower layer. The higher resistance the flow experienced at the bottom compared with the interface means, that the dynamic velocity of the lower layer necessary for producing the entrainment is less than that of the upper layer (approximately 2/3 of the upper layer velocity, see Bo Pedersen 1980a), which again agrees well with the observations in the Great Belt. Hence although the model is crude, it reflects the main hydrodynamic behaviour of the complex Belt-area.

12

Subarea 3: The Arkona Basin

The most characteristic hydrodynamic feature of the Arkona Basin can be observed during an inflow situation, where a dense bottom current is formed along the southern bank of the Basin. Passing the sills in the Great Belt and in the Sound the saline water flows into the Arkona Basin, where it very soon plunge down and descend to the deep water of the Bornholm Basin, i.e. below the interface located at approximately 45 m depth, see Fig. 1. During its course it entrains water from the less saline overlaying water, resulting in a decrease in salinity from 16‰ at the Darss Sill to about 11-12‰, at the merging with the lower layer in the Bornholm Basin. During a subsequent outflow situation the dense bottom current gradually runs dry and finally disappears until the process is repeated by a new inflow. The ambient water in the Arkona Basin is nearly homogeneous (except for the thermocline formation) because the average depth is less than the upper well-mixed layer of the adjacent Bornholm Basin. Hence the flow conditions in the upper layer of the Arkona Basin has no significant influence on the mixing of salt in the Baltic, and the salinity can therefore be taken as equal to the value present at the transition to the Bornholm Basin, namely 7.8‰.

The sparse measurements of the dense bottom current (Petrén et al. 1975), indicates an order of magnitude of typically 5 meter of the thickness of this current when present. If we apply Eq. (7) outlined in the previous chapter on the dense bottom current and takes the drop in elevation equal to the vertical distance from the plunge line to the interface in the Bornholm Basin ($y_{B0} = 45$ m) we get an average depth of $y_{A1} = 3.8$ m, in reasonable agreement with the observations. In these calculations we have applied the constant mass deficit flux condition

$$\Delta_{SA} Q_{SA1} = \Delta_B Q_{B1} \tag{23}$$

where indexes $SA1$ and $B1$ stand for the lower layers at the Darss Sill and at the Bornholm Basin respectively. A further condition necessary for the later calculations is Eq. (8) expressing the assumed constancy of the densimetric Froude number at the sill.

Subarea 4: The Bornholm Basin

The Bornholm Basin is a 80 to 100 m deep basin separated from the central Baltic Sea by a shallow sill with a narrow local depression to 60 m depth at the Stolpe Channel. The intermittent flow of dense water from the Arkona Basin is smoothed out and continues through the Stolpe Channel. Hence the lower layer in the Bornholm Basin only acts as a buffer for the discontinous inflow, with a retention time of say 10 weeks (Bo Pedersen 1977), while there is very little downwards directed mixing.

The position of the interface is determined by the rate of outflow through the Stolpe Channel. This flow is assumed to be governed by a constant densimetric Froude number, see Eq. (8). Hence the interfacial depth in the Bornholm Basin is

13

related to the depth y_{C1} of the dense bottom current present in the Stolpe Channel and to the sill depth (= 60 m) in the following way

$$y_{B0} = 60(m) - y_{C1}$$ (24)

The upper layer is exposed to the wind and the heating/cooling sequence, which as stated in the previous chapter gives rise to an upwards directed entrainment through the halocline during half of the year. Hence Eq. (3b) shall be modified to

$$\frac{V_E}{U_F} = 0.5 \frac{2.3 \ U_F^2}{\Delta g \ y_{B0}}$$ (25)

which yields a total discharge through the halocline of

$$Q_{EB0} = 1.5 \frac{U_F^3 A_B}{g(S_{B1} - S_{B0})y_{B0}}$$ (26)

Inserting $U_F \simeq 8 \times 10^{-3}$ m/s yields $Q_{EB} = 8.9 \times 10^3$ m^3/s in yearly average. The upper layer salinity S_{B0} can be found by applying the combined equation for transport of salt and volume through the Bornholm/Arkona section

$$S_{B0}(Q_{B1} + R) = S_{B1}Q_{B1}$$ (27)

A check on the calculated entrainment Q_{EB0} is that it is compatible with a salinity of $S_{\emptyset 0} = 7.0‰$ in the upper layer of the Central Baltic, in accordance with observations.

Subarea 5: The Stolpe Channel

Surbarea 5 has the same hydrodynamic status as subarea 3, the Arkona Basin, the only significant difference being, that the dense bottom current here is nearly steady. The continuity of volume yields an upstream discharge of

$$Q_{BC1} = Q_{B1} - Q_{EB0}$$ (28)

i.e. the bottom water inflow to the Bornholm Basin Q_{B1} reduced by the upwards directed entrainment Q_{EB0}.

The salinity has accordingly decreased slightly, confer with continuity equation for mass or salt deficit

$$Q_{BC1}(S_{B1} - S_{\emptyset 0}) = Q_{\emptyset 1}(S_{\emptyset 1} - S_{\emptyset 0})$$ (29)

which yields the salinity of inflowing bottom water to the Baltic Proper $S_{\emptyset 1} = 11‰$ in agreement with observations.

Similar to the Arkona bottom current the depth of the Stolpe Channel current is assumed to be governed by a constant densimetric Froude number at the head of the current.

14

Subarea 6: The Central Baltic

The Central Baltic Basin is the largest of the subareas and furthermore the deepest (up to about 400 m). The main inflows of fresh water to the system takes place here, comprising direct river runoff (31%), contribution from the Finnish Bay (27%) and from the Bothnian Bay (42%).

The nearly persistent brackish water flow from the Stolpe Channel descends to below the primary halocline, located at approximately 60 m depth, where it spreads out at the density-matching level. The continuity of the volume demands an upwards directed entrainment $Q_{E\emptyset}$, caused by the energy input from the wind and the cooling, both of which are kept unchanged in the present analysis. The combined effects of all the external forces can be integrated to a single representative dynamic friction velocity $U_{F\emptyset}$, yielding an entrainment of (see Eq. (26))

$$Q_{E\emptyset} = Q_{\emptyset 1} = \frac{1.5 \, A_{\emptyset} \, U_{F\emptyset}^{3}}{(S_{\emptyset 1} - S_{\emptyset 0}) g \, y_{\emptyset 0}} \tag{30}$$

Inserting the observed values gives a dynamic friction velocity of $U_{F\emptyset} \simeq 8 \times 10^{-3}$ m/s. Although this velocity compares well with the observed wind velocity, one has to remember that $U_{F\emptyset}$ contains the integrated effects of all the external forces and hence may be difficult to evaluate exactly, but as demonstrated, the order of magnitude is correct.

On an average, the upper layer of the Central Baltic is nearly homogeneous due to the multi-directed wind-driven circulations and the long retention time. The salinity is determined by the continuity equation for salt which states

$$S_{\emptyset 0} (R + Q_{\emptyset 1}) = S_{\emptyset 1} Q_{\emptyset 1} \tag{31}$$

Subareas 7 and 8: The Finnish Bay and The Bothnian Bay

The salinity distribution and the position of the interface in the two subareas are governed by the boundary conditions, which, besides the external forces, are the fresh water input and the conditions in the Central Baltic, respectively. A change in these boundary conditions will have a measurable effect on the hydrography of both Bays' – but it will not influence the conditions in the Central Baltic – besides the changes caused by the change in the fresh-water input. Hence, as we are mainly concerned with the Central Baltic and the Danish Inland waters, a detailed analysis or modelling of the Finnish Bay and the Bothnian Bay is omitted. Another reason for not taking the two Bays into account is, that major changes may take place in the Finnish Bay which make the linearized approach doubtful.

15

The Consequence Analysis

The equations outlined in the previous chapters give an overall quantitative description of the Baltic estuary system, as it behaves under the present average meteorologic and hydrographic conditions. A man-made change in the runoff from the river Neva has of course a direct influence on the total fresh-water inflow to the Baltic, while it is unlikely to have any significant influence on the meteorological conditions and hence on the external forces. Therefore, the conditions before and after the river diversion both satisfies the outlined governing equations. Furthermore, the changes are relatively small, which suggests a linearization of the equations. The procedure is to introduce the new parameters as the old ones plus a minor correction, as for instance

$$
\begin{aligned}
R_{new} &= R(1 + r) \\
Q_{new} &= Q(1 + q) \\
S_{new} &= S(1 + s) \\
y_{new} &= y(1 + \eta) \\
\lambda_{new} &= \lambda(1 + \ell)
\end{aligned}
\tag{32}
$$

where r, q, s, η and λ all are small dimensionless quantities. By use of a Taylor expansion in which only the first order terms are retained, a set of linear equations in the correction terms is obtained, which can be solved directly. The original as well as the linearized equations are for conveniency summarized in Table 1, where the solution to the set of equations is shown as well. In the linearized equations due respect to the changes in the interfacial widths or areas with depth have been taken.

All the corrections have been related to the fresh-water discharge reduction r in the data output. Hence – as an example – if the fresh-water diversion from the river Neva amounts to 5 per cent of the total fresh-water inflow to the Baltic (i.e. approximately 25 per cent reduction of the river Neva's discharge), then $r = - 0.05$. By use of Table 1 the associated changes in the salinities, depths and discharges can be evaluated. Some of the calculated changes can be compared with the natural variations encountered in the Baltic estuary system during this century. We have chosen to illustrate this variability by plotting the 10-year sliding mean values of the runoff R from river Vuoksi, the salinity $S_{\varnothing 0}$ and the depth $y_{\varnothing 0}$ in the upper layer in the Central Baltic and finally the upper layer salinity in the Cattegat region, see Fig. 5. Two comments to this illustration are appropriate. First, the natural variations are caused by the combined effects of a variability in the runoff and in the climate, the last one being held unchanged in our calculations. Second, the natural variations are highly non-steady, while our analysis deals with the steady state. In the non-steady case, the reservoir effect damps the amplitudes of a cyclic variation (as for instance in the salinity) compared to the long-term response of a step function and furthermore the output is delayed compared to the time

16

TABLE 1

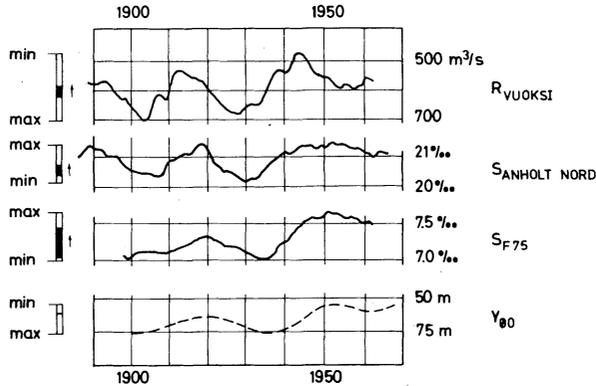| EQT. No	THE GOVERNING EQUATIONS	REGION	THE LINEARIZED EQUATIONS	SOLUTION
14	$B^2 y_{K0}^3 (33 \cdot 10^{-3} - S_{MK0}) = 9.44 \cdot 10^{10}$		$1.80 n_{K0} - 2.37 s_{MK0} = 0$	$n_{K0} = -0.36\,r$
18	$(33 \cdot 10^{-3} - S_{MK0}) = (33 \cdot 10^{-3} - S_{KS0}) \exp(-\frac{240 \cdot 10^3 m}{\lambda_K})$	K	$-2.37 s_{MK0} + 1.20 s_{KS0} - 0.43 \ell_K = 0$	$s_{MK0} = -0.27\,r$
16	$\lambda_K = 1.81 \cdot 10^5 \frac{R y_{K0}}{B_K}$		$-\ell_K + 1.60 n_K = -r$	$s_{KS0} = -0.39\,r$
	$B_K = 64 \cdot 10^3 (1 - 0.6 n_{K0})$			$\ell_K = 0.42\,r$
21	$Q_{SA1} + R = 2.92 \cdot 10^4\ [m^3/s]$		$-1.42 q_{SA1} = 1.50\,r$	$q_{SA1} = -1.06\,r$
22	$S_{KS0}(Q_{ES0} - Q_{ES1} + Q_{SA1} + R) = 33 \cdot 10^{-3}(Q_{ES0} - Q_{ES1} + Q_{SA1})$		$s_{KS0} - 0.69 q_{ES0} + 0.59 q_{ES1} - 0.36 q_{SA1} = -0.46\,r$	$q_{ES0} = -0.03\,r$
23	$S_{SA1} Q_{SA1} = (Q_{ES0} - Q_{ES1} + Q_{SA1}) 33 \cdot 10^{-3} - Q_{ES0} S_{S1} + Q_{ES1} S_{S0}$	S	$s_{SA1} - 1.06 q_{SA1} - 1.02 q_{ES0} + 2.07 q_{ES1} + 2.93 s_{S1} - 1.33 s_{S0} = 0$	$q_{ES1} = -0.81\,r$ $s_{SA1} = 0.04\,r$
24	$S_{S0} = 0.5(S_{KS0} + S_{B0})$ $S_{S1} = 0.5(33 \cdot 10^{-3} + S_{SA1})$		$s_{S0} - 0.70 s_{KS0} - 0.30 s_{B0} = 0$ $s_{S1} - 0.33 s_{SA1} = 0$	$s_{S1} = 0.01\,r$ $s_{S0} = -0.33\,r$
8	$Q_{ES0} = \frac{4.20 \cdot 10^3}{(S_{S1} - S_{S0}) y_{K0}}$		$q_{ES0} + 1.0 n_{K0} + 2.11 s_{S1} - 1.11 s_{S0} = 0$	
9	$Q_{ES1} = \frac{3.22 \cdot 10^3}{(S_{S1} - S_{S0})(25 - y_{K0})}$		$q_{ES1} - 1.14 n_{K0} + 2.11 s_{S1} - 1.11 s_{S0} = 0$	
26	$(S_{SA1} - S_{B0}) Q_{SA1} = (S_{B1} - S_{B0}) Q_{B1}$		$1.95 s_{SA1} + 1.28 s_{B0} + q_{SA1} - q_{B1} - 3.23 s_{B1} = 0$	
10	$Q_{B1} = Q_{SA1} \exp\{0.072 \frac{y_{B0}}{y_{A1}}\}$	A	$q_{B1} - q_{SA1} + 0.85 n_{A1} - 0.85 n_{B0} = 0$	$n_{A1} = -0.79\,r$
11	$\frac{Q_{SA1}^2}{(S_{SA1} - S_{B0}) y_{A1}^3} = 4.48 \cdot 10^8$		$2 q_{SA1} - 1.95 s_{SA1} + 0.95 s_{B0} - 3 n_{A1} = 0$	
27	$y_{B0} = 60[m] - y_{C1}$		$3 n_{B0} + n_{C1} = 0$	$s_{B0} = 0.16\,r$
29	$Q_{EB0} = \frac{7.79 \cdot 10^{-8} A_B}{(S_{B1} - S_{B0}) y_{B0}}$	B	$q_{EB0} + 1.60 n_{B0} + 3.23 s_{B1} - 2.23 s_{B0} = 0$	$s_{B1} = -0.31\,r$ $n_{B0} = 0.16\,r$
30	$S_{B0}(Q_{B1} + R) = S_{B1} Q_{B1}$ $A_B = 1.8 \cdot 10^{10}(1 - 0.6 n_{B0})$		$s_{B0} - s_{B1} + 1.69 q_{B1} = -0.31\,r$	$q_{B1} = -0.25\,r$ $q_{EB0} = 0.29\,r$
31	$Q_{BC1} = Q_{B1} - Q_{EB0}$		$q_{BC1} - 1.36 q_{B1} + 0.36 q_{EB0} = 0$	$n_{C1} = -0.48\,r$
32	$Q_{BC1}(S_{B1} - S_{\phi0}) = Q_{\phi1}(S_{\phi1} - S_{\phi0})$	C	$q_{BC1} - q_{\phi1} + 2.63 s_{B1} + 0.12 s_{\phi0} - 2.75 s_{\phi1} = 0$	$q_{BC1} = -0.44\,r$
11	$\frac{Q_{BC1}^2}{(S_{B1} - S_{\phi0}) y_{C1}^3} = 4.10 \cdot 10^7$		$2 q_{BC1} - 2.63 s_{B1} + 1.63 s_{\phi0} - 3 n_{C1} = 0$	
10	$Q_{\phi1} = Q_{BC1} \exp\{0.072 \frac{y_{\phi0} - y_{B0}}{y_{C1}}\}$		$q_{\phi1} - q_{BC1} - 0.29 n_{\phi0} + 0.22 n_{B0} + 0.07 n_{C1} = 0$	
33	$Q_{\phi1} = \frac{7.89 \cdot 10^{-8} A_\phi}{(S_{\phi1} - S_{\phi0}) y_{\phi0}}$		$q_{\phi1} + 2.1 n_{\phi0} + 2.75 s_{\phi1} - 1.75 s_{\phi0} = 0$	$q_{\phi1} = -0.46\,r$
34	$S_{\phi0}(R + Q_{\phi1}) = S_{\phi1} Q_{\phi1}$ $R = 1.5 \cdot 10^4 m^3/s$	Ø	$s_{\phi0} - 0.36 q_{\phi1} - s_{\phi1} = -0.36\,r$	$s_{\phi0} = -0.85\,r$ $s_{\phi1} = -0.33\,r$
	$A_\phi = 8 \cdot 10^{10}(1 - 1.1 n_{\phi0})$			$n_{\phi0} = -0.06\,r$

Fig. 5. The secular changes in the Baltic Sea estuary system illustrated by the 10-year sliding mean of the runoff from river Vuoksi (Nilsson and Svansson 1974), the surface salinity at Anholt Nord (Nilsson and Svansson 1974), the upper layer salinity at station F75 (the Central Baltic, Hela 1966), the upper layer depth in the Central Baltic (Fonselius 1969).
In the column diagram to the left is shown the min/max values observed and the changes calculated for a 25 per cent reduction of the river Neva's runoff.

for the input. The time delaying effect is demonstrated in the salinity observed at station F75, which shows a response time of about 10 years, compatible with the retention time in the upper layer of the Central Baltic. A throughout discussion of the observed data shall not be given, mostly due to lack of knowledge of the variability in the meteorologic forcing. Instead we shall compare and comment upon the natural and man-made variations as observed and calculated, respectively.

The man-made reduction in our example is 5% of the total runoff to the Baltic. This reduction is an order of magnitude less than the natural variations encountered during this century as represented by the runoff of river Vuoksi, see Fig. 5.

The most pronounced influence of a man-made reduction in the runoff is to be found in the upper layer salinity in the Central Baltic, see Fig. 5, S_{F75}, where the calculated salinity change is approximately half the variation observed during this century. The observed salinity variations reflects the non-steady input from fresh water (R) and wind (U_F), and are therefore highly damped by the reservoir effect, as compared to the values one would have had if a permanent change in R and U_F had occurred. Moreover the observed salinity is highly influenced by the change in the meteorological conditions, which are not taken into account in our calculations. Therefore, the relatively strong influence of a man-made change in the runoff is understandable.

The change in salinity of the upper layer of the Cattegat light-vessel Anholt Nord is only approximately 20% of the natural maximum variation observed. In

fact the 10-year sliding mean is a bad representation of the salinities in the Cattegat region because the retention time is orders of magnitude less. Compared to the more representative month sliding mean the influence is reduced to less than say 5% of the natural variations.

Finally we found a negligible change in the upper layer depth of the Central Baltic. The actual maximum change has been about 20%. Hence the position of the interface in the Central Baltic is primarily determined by the changes in the meteorological conditions, which have an influence directly in determining the rate of entrainment and indirectly in determining the sill overflow and hence the discharge into the lower layer.

Conclusion

The possible influence on the hydrography of the Baltic Sea estuary system subject to a man-made change in the river runoff, has been investigated. The density stratification, the geometry and the variability of the external forces makes the estuary a rather complex hydrodynamic system and hence it was necessary to divide it into eight subareas, each of which described by its own balance in mass, volume and dynamic (mixing). It has been demonstrated that the prevailing meteorological conditions over the area play the dominating role in the formation of fronts, salt water wedges, dense bottom currents and all the other types of density currents encountered in the system and in the mixing processes. These meteorological conditions are kept unchanged in the present consequence analysis, which has been performed by linearizing the governing equations with respect to the minor changes caused by the man-made change in the river Neva's runoff. The changes in the depths, discharges and salinities in the system have been presented as functions of the change in the fresh-water discharge. Although it is not the intention of this paper to reach any conclusions concerning the possible positive or negative consequences of the river diversion it shall be emphasized, that the dynamic stability of the estuary system will be reduced, which makes the system more sensitive to the inevitable changes in the external forces, i.e. in the natural variations in the meteorology. This reduced stability is caused by the combined effects of an increased salinity and a decreased upper layer depth.

The salinity increase in the upper layer of the Central Baltic is remarkably large compared to the natural variations encountered during this century. The reason for this is the reservoir effect, which highly damps a cyclic variation (the natural) but not a step-variation (the man-made).

19

References

Bo Pedersen, Fl. (1977) On dense bottom currents in the Baltic Deep Water. *Nordic Hydrology,* 8, 297-316.

Bo Pedersen, Fl. (1978) On the influence of a bridge across the Great Belt on the hydrography of the Baltic Sea, 11th conference of the Baltic Oceanographers, Rostock, DDR.

Bo Pedersen, Fl. (1980a) A monograph on turbulent entrainment and friction in two-layer stratified flow. Series Paper No. 25, Inst. of Hydrodynamics and Hydraulic Eng., Tech. Univ. of Denmark.

Bo Pedersen, Fl. (1980b) Dense bottom currents in Rotating Ocean. American Society of Civil Engineers, *Proc. Vol. 106, Hy 8,* 1291-1308.

DHI-Report (1977) Bæltprojektet. Matematiske modeller af Store Bælt og Øresund – Slutrapport. Dansk Hydraulisk Inst. DK-2970 Hørsholm.

Fonselius, S. H. (1969) Hydrography of the Baltic Deep Basins III, Fishery Board of Sweden, Series Hydrography, Report No. 23.

Golubev, G. (1978) Environmental Issue of Large Interregional Water Transfer Projects. *Water Supply and Management, Vol. 2,* 177-185.

Hela, I. (1966) Secular changes in the salinity of the upper waters of the Northern Baltic Sea. *Commentationes Physico-Mathematicae, Vol. 31,* Nr. 14, 1966.

Jacobsen, T. (1980) Sea Water exchange of the Baltic. Measurements and methods. Preprint of Dr. thesis. Inst. of Physical Oceanography. Univ. of Copenhagen.

Mikhaylov, N. I., Nikolayev, V. A., and Timashev, I. Ye. (1977) Environmental Protection Issue and Southward Diversion of Siberian Rivers. English Translation from: Vestnik Moskovskog Universiteta, Geografiya (1977), No. 5, pp. 50-56.

Møller, Jacob Steen (1980) Østersøens Hydrografi. Internal Report in Danish. Inst. of Hydrodynamics and Hydraulic Eng. Tech. Univ. of Denmark.

Nilsson, H., and Svansson, A. (1974) Long term variations of Oceanographic Parameters in the Baltic and Adjacent Waters. Meddelande från Havsfiske-laboratoriet, Lysekil, nr. 174.

Petrén, O., and Walin, G. (1975) Some observations of the deep flow in the Bornholm strait during the period June 73 – December 74, Rep. No. 12, Inst. of Oceanography, Univ. of Gothenburg, Sweden.

Rydberg, L. (1976) Observations of the deep water flow through the Stolpe Channel during August 1976. Rep. No. 15. Inst. of Oceanography, Univ. of Gothenburg, Sweden.

The Beltproject (1976) Interim report on the Danish Belt project (In Danish). Publ. by Miljøstyrelsen, Kampmannsgade 1, DK-1604 Copenhagen.

Voropaev, G. V. (1978) The Scientific Principles of Large-Scale Areal Redistribution of Water Resources in the USSR. *Water Supply and Management, Vol. 2,* pp. 91-101.

Address:
Institute of hydrodynamics and hydraulic engineering,
ISVA,
Technical University of Denmark,
Building 115,
DK-2800 Lyngby, Denmark.